

TGF- β -FOXO signalling maintains leukaemia-initiating cells in chronic myeloid leukaemia

著者	Naka Kazuhito, Hoshii Takayuki, Muraguchi Teruyuki, Tadokoro Yuko, Ooshio Takako, Kondo Yukio, Nakao Shinji, Motoyama Noboru, Hirao Atsushi
journal or publication title	Nature
volume	463
number	7281
page range	676-680
year	2010-02-04
URL	http://hdl.handle.net/2297/23898

doi: 10.1038/nature08734

1 TGF- β -FOXO signalling maintains leukaemia-initiating cells in chronic myeloid leukaemia

Kazuhito Naka^{1*}, Takayuki Hoshii^{1*}, Teruyuki Muraguchi¹, Yuko Tadokoro¹, Takako Ooshio^{1,2}, Yukio Kondo³, Shinji Nakao³, Noboru Motoyama⁴ & Atsushi Hirao^{1,2}

Chronic myeloid leukaemia (CML) is caused by a defined genetic abnormality that generates *BCR-ABL*, a constitutively active tyrosine kinase¹. It is widely believed that *BCR-ABL* activates Akt signalling that suppresses the forkhead O transcription factors (FOXO), supporting the proliferation or inhibiting the apoptosis of CML cells²⁻⁴. Although the use of the tyrosine kinase inhibitor imatinib is a breakthrough for CML therapy, imatinib does not deplete the leukaemia-initiating cells (LICs) that drive the recurrence of CML⁵⁻⁸. Here, using a syngeneic transplantation system and a CML-like myeloproliferative disease mouse model, we show that Foxo3a has an essential role in the maintenance of CML LICs. We find that cells with nuclear localization of Foxo3a and decreased Akt phosphorylation are enriched in the LIC population. Serial transplantation of LICs generated from *Foxo3a*^{+/+} and *Foxo3a*^{-/-} mice shows that the ability of LICs to cause disease is significantly decreased by Foxo3a deficiency. Furthermore, we find that TGF- β is a critical regulator of Akt activation in LICs and controls Foxo3a localization. A combination of TGF- β inhibition, Foxo3a deficiency and imatinib treatment led to efficient depletion of CML *in vivo*. Furthermore, the treatment of human CML LICs with a TGF- β inhibitor impaired their colony-forming ability *in vitro*. Our results demonstrate a critical role for the TGF- β -FOXO pathway in the maintenance of LICs, and strengthen our understanding of the mechanisms that specifically maintain CML LICs *in vivo*.

Although tyrosine kinase inhibitor (TKI) therapy of CML patients efficiently induces the death of leukaemia cells⁵⁻⁸, LICs in these patients can survive this therapy. To understand the molecular mechanisms maintaining CML LICs, we characterized LICs *in vivo* using a mouse model for CML-like myeloproliferative disease (MPD)⁹. Consistent with previous reports¹⁰⁻¹³, we found that a rare c-Kit⁺Lineage⁻(Lin⁻)Sca-1⁺ (KLS⁺) population of CML cells (that is, bearing markers of normal haematopoietic stem cells (HSCs)) induced efficient CML development in recipient mice (Supplementary Fig. 1). In contrast, neither c-Kit⁺Lin⁻Sca-1⁻ (KLS⁻) cells (which correspond to normal progenitors), nor other CML cell populations expressing differentiation markers, induced CML.

We and others have shown that Foxo transcription factors, which are important downstream targets of PI3K-Akt signalling, are essential for the maintenance of self-renewal capacity in normal HSCs¹⁴⁻¹⁶. When a growth factor binds to the appropriate receptor, Akt is activated and phosphorylates Foxo proteins, resulting in their nuclear export and subsequent degradation in the cytoplasm. In the absence of growth factor stimulation, Foxo proteins are retained in an active state in the nucleus and induce their transcriptional targets. In CML cell lines, *BCR-ABL* is thought to activate PI3K-Akt signalling that leads to nuclear

export of Foxo factors and suppression of their transcriptional activity²⁻⁴. However, we found that, whereas most KLS⁻ cells (non-LICs) showed the expected cytoplasmic localization of Foxo3a, KLS⁺ cells (LICs) enriched cells with nuclear localization of Foxo3a (Fig. 1a and Supplementary Fig. 2), as observed in normal HSCs^{15,17} (Supplementary Fig. 3). LICs with nuclear Foxo3a also exhibited decreased levels of phosphorylated Akt (p-Akt) compared to most non-LICs, suggesting that Foxo3a remains active in LICs owing to Akt suppression.

We next examined the role of Foxo3a in CML initiation by establishing *Foxo3a*-deficient CML model. We isolated immature bone marrow cells from *Foxo3a*^{+/+} and *Foxo3a*^{-/-} littermates¹⁵, infected these cells with retrovirus carrying the *BCR-ABL* gene, and transplanted them into syngeneic recipients (first bone marrow transplantation (BMT)). Both recipient groups showed the same symptoms of CML-like MPD, including increased myeloid cells in peripheral blood and splenomegaly⁹ (Fig. 1b, c, left and Supplementary Figs 4 and 5). Thus, Foxo3a was dispensable for the generation of CML-like disease. After a first BMT, the absolute numbers of *Foxo3a*^{-/-} LICs in recipient spleen and bone marrow were significantly higher than the absolute numbers of *Foxo3a*^{+/+} LICs present in recipient organs (Fig. 1d, left and Supplementary Fig. 6a), although the *in vitro* colony-forming ability of these *Foxo3a*^{+/+} and *Foxo3a*^{-/-} LICs was comparable (Fig. 1e, left).

When we transplanted *Foxo3a*^{+/+} and *Foxo3a*^{-/-} LICs from first BMT mice into a new set of recipients (second BMT), there was no difference in CML development (Fig. 1b, c, centre and Supplementary Figs 4 and 5). However, the *in vitro* colony-forming ability of second BMT LICs was decreased by loss of *Foxo3a* (Fig. 1e, right). In a third BMT, relatively mild CML-like MPD developed in recipients within one month. Foxo3a deficiency prevented the propagation of CML cells in the peripheral blood and spleen *in vivo* (Fig. 1b, right and Supplementary Figs 4 and 5). Furthermore, the absolute numbers of *Foxo3a*^{-/-} LICs in the organs of third BMT recipients were much lower than in third BMT recipients that had received *Foxo3a*^{+/+} LICs (Fig. 1d, right and Supplementary Fig. 6). Thus, *Foxo3a*^{-/-} LICs may retain sufficient function to cause disease in second BMT recipients but succumb to exhaustion in third BMT recipients. Although CML-like MPD developed in mice that had received either *Foxo3a*^{+/+} or *Foxo3a*^{-/-} LICs within 40 days of a third BMT (Supplementary Fig. 5a, b), recipients of *Foxo3a*^{+/+} LICs also developed acute lymphocytic leukaemia (ALL), as well as CML, 40 days after the third BMT (Supplementary Fig. 5c) as reported¹⁸, suggesting that these LICs can generate malignancies in several lineages. Notably, we did not observe development of ALL or CML in recipients of *Foxo3a*^{-/-} LICs 45 days after a third BMT (Supplementary Fig. 5c), suggesting that the *Foxo3a*^{-/-} LICs lose their potential to generate malignancies. This

¹Division of Molecular Genetics, Center for Cancer and Stem Cell Research, Cancer Research Institute, Kanazawa University, Kanazawa, Ishikawa 920-0934, Japan. ²Core Research for Evolution Science and Technology (CREST), Japan Science and Technology Agency (JST), Chiyoda-ku, Tokyo 102-0075, Japan. ³Cellular Transplantation Biology, Division of Cancer Medicine, Kanazawa University, Graduate School of Medical Science, Kanazawa, Ishikawa 920-8641, Japan. ⁴Department of Geriatric Medicine, National Institute for Longevity Sciences, National Center for Gerontology and Geriatrics, 36-3 Gengo, Morioka, Obu, Aichi 474-8522, Japan.

*These authors contributed equally to this work.

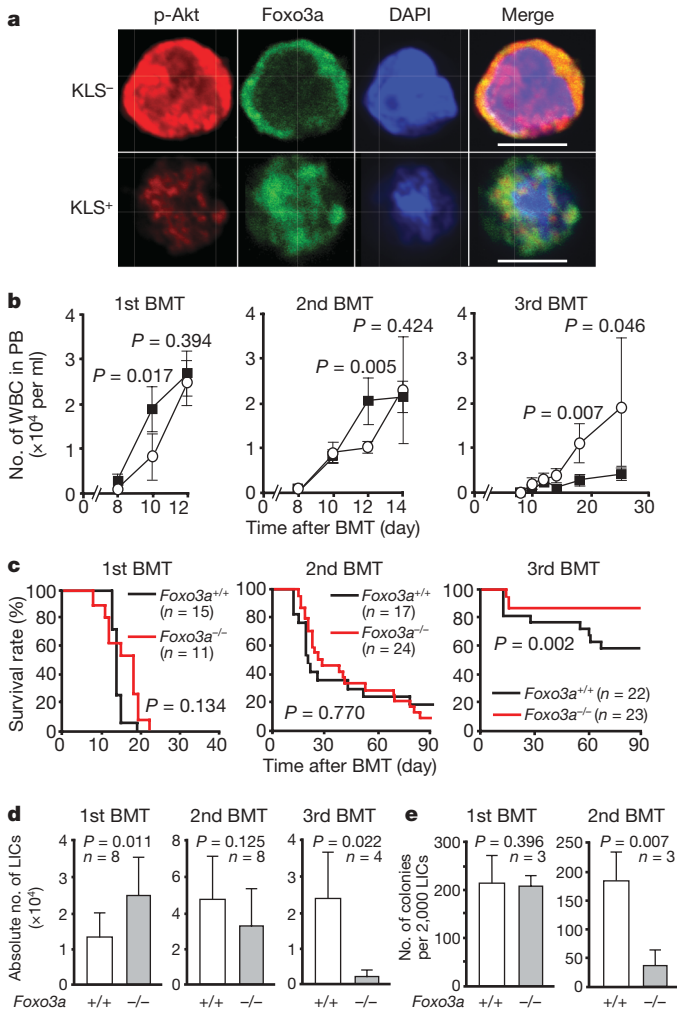


Figure 1 | Maintenance of CML LICs depends on Foxo3a. **a**, Decreased Akt phosphorylation and increased Foxo3a nuclear localization in CML LICs. BCR-ABL-GFP⁺ KLS⁻ and KLS⁺ cells were immunostained to detect p-Akt and Foxo3a. Nuclei were visualized using 4',6-diamidino-2-phenylindole (DAPI; blue). Scale bars, 10 μm. **b**, Numbers of white blood cells (WBC) in peripheral blood (PB) in *Foxo3a*^{+/+} (open circles) and *Foxo3a*^{-/-} (closed squares) CML-affected mice at first to third BMT. Data shown are the mean WBC number ± s.d. (n = 4). **c**, **d**, Survival rate (**c**) and absolute number of LICs (**d**) in CML-affected mice. Data are expressed as percentage survival (**c**) and absolute number of LICs ± s.d. in spleen (**d**). **e**, *In vitro* colony-forming ability of LICs. Data shown are the mean colony number ± s.d.

inability of *Foxo3a*^{-/-} LICs to induce or sustain leukaemia resulted in the reduced lethality of these animals (Fig. 1c, right). Thus, Foxo3a is essential for the long-term maintenance of leukaemia-initiating potential. Because the introduction of a dominant-negative Foxo moiety into CML LICs impaired LIC function *in vivo* (Supplementary Fig. 7), the defective maintenance of *Foxo3a*^{-/-} LICs is probably due to a diminution in LIC self-renewal activity rather than a defect in the original HSCs. Furthermore, the Foxo4 protein expression pattern in LICs is very similar to that of Foxo3a (Supplementary Fig. 8), suggesting an overlap in Foxo functions.

We next determined how Foxo3a deficiency impaired the maintenance of the CML-initiating potential of LICs. Loss of *Foxo3a* did not affect LIC differentiation potential (Fig. 2a) or cell cycle status (Fig. 2b), although LICs with nuclear localization of Foxo3a showed lower expression of the Ki67 antigen (Supplementary Fig. 9). However, TdT-mediated dUTP nick end labelling (TUNEL)-positive apoptotic cells were significantly increased in histological sections of bone marrow and spleen from *Foxo3a*^{-/-} CML-affected mice

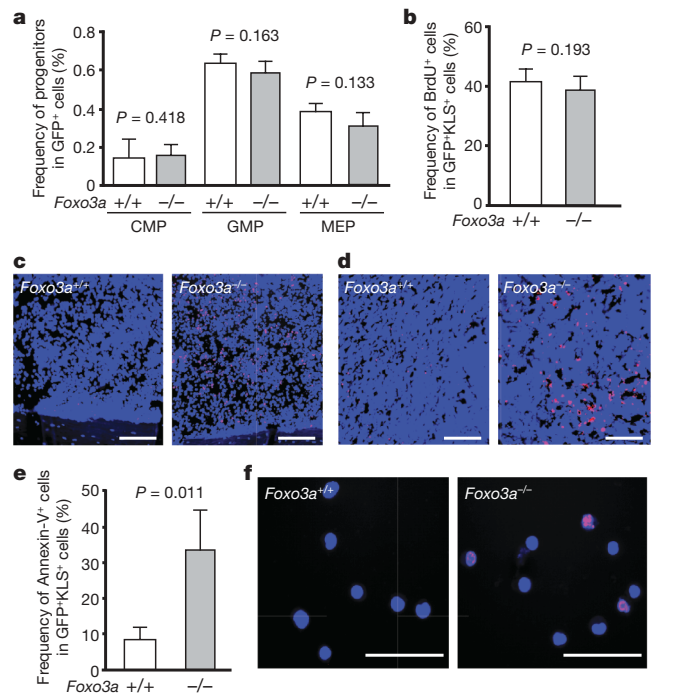


Figure 2 | Essential role of Foxo3a in suppression of LIC apoptosis.

a, **b**, Comparable differentiation potential and cell cycle status *in vivo*. **a**, Data show the mean percentage ± s.d. of CMP (common myeloid progenitors)-, GMP (granulocyte-macrophage progenitors)-, and MEP (megakaryocyte-erythroid progenitors)-like cells in BCR-ABL-GFP⁺ bone marrow cells (n = 3). **b**, Data are the mean frequency of BrdU⁺ cells ± s.d. (n = 3). **c**–**f**, Increased apoptosis of *Foxo3a*^{-/-} LICs. **c**, **d**, Histological sections of bone marrow (**c**) and spleen (**d**) from *Foxo3a*^{+/+} or *Foxo3a*^{-/-} CML-affected mice at second BMT were analysed by TUNEL staining (red) and DAPI. Scale bars, 100 μm. **e**, Mean percentage ± s.d. of Annexin-V⁺ cells among GFP⁺KLS⁺ cells (n = 3). **f**, LICs were subjected to TUNEL staining. Scale bars, 50 μm.

compared to controls (Fig. 2c, d). To confirm that this apoptosis was occurring in LICs, we purified KLS⁺ cells and showed that the frequency of Annexin-V⁺ or TUNEL⁺ cells among *Foxo3a*^{-/-} KLS⁺ cells was higher than among *Foxo3a*^{+/+} KLS⁺ cells (Fig. 2e, f). Thus, Foxo3a is required for LIC survival because it mediates suppression of apoptosis.

An intriguing question in current CML research is how Akt is inactivated (and thus Foxo is activated) mainly in LICs, despite BCR-ABL expression in all CML cells. The fact that TGF-β regulates Akt activation (and thus nuclear Foxo3a) in normal HSCs prompted us to assess whether TGF-β signalling controls Foxo localization in CML LICs¹⁹. We first examined the phosphorylation of Smad2/3 proteins, which are downstream effectors in the TGF-β signalling pathway²⁰. Phosphorylation of Smad2/3 in the nuclei of CML KLS⁺ cells was higher than that in KLS⁻ cells (Fig. 3a and Supplementary Fig. 10), indicating that TGF-β signalling was activated in CML LICs. We then treated CML KLS⁺ cells *in vitro* for 2 h with either TGF-β1 or the TGF-β inhibitor Ly364947 (ref. 21) and analysed Foxo3a localization. TGF-β1 treatment increased Foxo3a nuclear localization, whereas Ly364947 promoted nuclear export of Foxo3a (Fig. 3b–d and Supplementary Fig. 11). Furthermore, KLS⁺ cells treated with TGF-β1 showed high Smad2/3 and low Akt phosphorylation levels, whereas cells treated with Ly364947 exhibited the opposite pattern (Fig. 3b, c and Supplementary Figs 11 and 12). The activity of mTOR complex 1 (mTORC1), which was determined by assessing the phosphorylation of S6 ribosomal protein²², correlated positively with p-Akt levels in these KLS⁺ cells (Fig. 3d and Supplementary Fig. 13). We propose that TGF-β signalling controls Akt activity in LICs, leading to retention of Foxo3a in the nucleus.

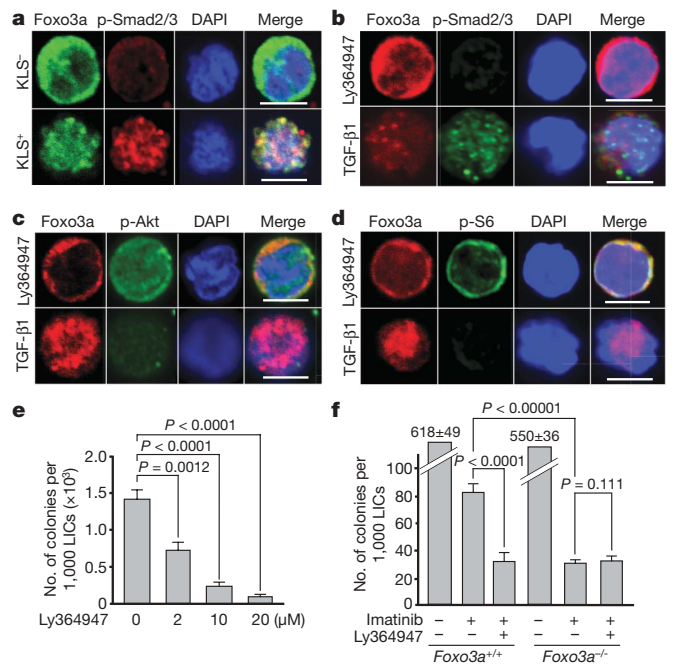


Figure 3 | TGF- β -Foxo signalling is required for the colony-forming capacity of LICs. **a**, Increased Smad2/3 phosphorylation in LICs. *Foxo3a*^{+/+} KLS⁺ and KLS⁻ CML cells were immunostained to detect Foxo3a and phosphorylated-Smad2/3 (p-Smad2/3). **b–d**, Control of Foxo3a localization by TGF- β signalling. LICs were treated *in vitro* with TGF- β 1 or Ly364947 for 2 h followed by immunostaining to detect Foxo3a and **(b)** p-Smad2/3, **(c)** p-Akt or **(d)** phosphorylated-S6 (p-S6). Scale bars, 10 μ m. **e**, Inhibition of TGF- β decreases LIC colony-forming ability. Representative data shown are the mean LIC colony number \pm s.d. ($n = 3$). **f**, TGF- β inhibition or Foxo3a deficiency enhances imatinib-mediated inhibition of LIC colony-forming capacity. Representative data shown are the mean colony number \pm s.d. ($n = 3$).

Notably, as TGF- β did not efficiently induce nuclear localization of Foxo3a in non-LICs (KLS⁻) cells (Supplementary Figs 14–16), there seem to be differences in how TGF- β -stimulated Foxo3a activation is regulated in LICs and non-LICs.

These findings led us to evaluate the effects of inhibition of TGF- β -Foxo signalling on the CML-initiating potential of LICs. Interestingly, TGF- β inhibitors (Ly364947, SD208) suppressed LIC colony-forming ability after co-culture with OP-9 stromal cells, which are used to maintain normal HSCs *ex vivo* and mimic their *in vivo* environment²³ (Fig. 3e and Supplementary Fig. 17a). Furthermore, although imatinib treatment alone of LICs co-cultured with OP-9 cells reduced the colony-forming capacity of *Foxo3a*^{+/+} CML LICs, the addition of TGF- β inhibitor significantly enhanced the inhibitory effect of imatinib on LIC colony-forming ability (Fig. 3f and Supplementary Figs 17b, c and 18a), consistent with a report in which TGF- β inhibition enhanced imatinib-induced cell death²⁴. Although Foxo3a deficiency alone did not affect LIC colony-forming ability (Fig. 1e, left), significantly fewer colonies arose from *Foxo3a*^{-/-} LICs treated with imatinib compared to treated *Foxo3a*^{+/+} LICs (Fig. 3f). When imatinib was combined with Foxo3a deficiency and Ly364947, there was no further inhibitory effect compared to either Foxo3a deficiency or Ly364947 treatment alone (Fig. 3f). TGF- β inhibition had no effect on the colony-forming ability of normal KLS⁺ cells under the same experimental conditions (Supplementary Fig. 18b). These data indicate that Foxo3a is an important downstream effector in the TGF- β signalling pathway driving the survival of LICs exposed to TKI therapy, and that inhibition of Foxo or TGF- β may be a highly useful adjunct to TKI therapy.

To test this hypothesis *in vivo*, we administered imatinib to second BMT mice bearing *Foxo3*^{+/+} or *Foxo3a*^{-/-} CML LICs. Without

imatinib, 80% of both groups died within 60 days (Fig. 4a). Administration of imatinib alone delayed CML onset and reduced recipient lethality, but 60% of the treated mice that had received *Foxo3a*^{+/+} LICs died within 90 days. In contrast, imatinib combined with Foxo3a deficiency significantly increased the survival of CML-affected mice. Moreover, when we isolated the residual KLS⁺ populations from these imatinib-treated recipients, we found that Foxo3a deficiency had reduced both the number and colony-forming ability of these LICs (Supplementary Fig. 19). Thus, Foxo3a is essential for the ability of CML LICs to survive imatinib therapy.

We then investigated the *in vivo* effect of a TGF- β inhibitor on LIC functions. Administration of Ly364947 alone led to increased p-Akt levels and decreased nuclear Foxo3a in LICs (Fig. 4b and Supplementary Fig. 20), demonstrating that TGF- β is a critical regulator of Akt and Foxo in LICs *in vivo*. Unlike the suppressive effect exerted by TGF- β *in vitro*, administration of Ly364947 alone did not extend the survival of second BMT *Foxo3a*^{+/+} mice with overt CML. However, Ly364947 combined with imatinib significantly reduced recipient lethality, decreased CML infiltration in lung (Fig. 4c and Supplementary Fig. 21a), and decreased LIC frequency (Supplementary Fig. 21b, c). These *in vivo* data suggest that CML LICs are more sensitive than normal HSCs/progenitors to TGF- β inhibitors.

Finally, we further confirmed that the suppressive effects of TGF- β inhibitors on mouse CML LIC function are also observed in human CML LICs. We isolated CD34⁺CD38⁻Lin⁻ cells as human CML LICs¹² from bone marrow cells of human CML patients, and co-cultured them on OP-9 cells with or without Ly364947. Ly364947 reduced the number of colonies formed by human CML LICs (Fig. 4d) and enhanced the inhibitory effects of imatinib on human CML LICs (Fig. 4e), suggesting that TGF- β -FOXO signalling also governs the behaviour of human CML LICs.

Our study indicates a model in which Foxo3a has opposite effects on the survival of LICs and non-LICs (Fig. 4f and Supplementary Discussion 1). In non-LICs, BCR-ABL drives strong Akt activation that forcefully represses Foxo3a functions. When TKIs block BCR-ABL and reduce Akt activation, activation of Foxo3a leads to apoptosis or cell cycle arrest. In contrast, in LICs, Akt activity is suppressed despite BCR-ABL expression *in vivo*, leading to nuclear localization of Foxo3a. Although a previous study suggested that Foxo3a may contribute to the acquisition of dormancy in leukaemia cells after exposure to anti-leukaemic agents², our data demonstrate that LICs have properties that allow them to resist various stress *in vivo* in a Foxo-dependent manner. Notably, we found that the role of Foxo3a in a CML blast crisis model was different from that in this MPD model (Supplementary Figs 22 and 23), indicating that Foxo proteins can mediate different regulatory mechanisms in different phases and types of leukaemia.

It remains unclear precisely how Akt and Foxo signalling is controlled in LICs *in vivo*. The presence of TGF- β 1 in CML LICs (Supplementary Fig. 24) and the *in vitro* effects of TGF- β inhibitor on Foxo3a localization in LICs suggest that a cell-autonomous effect of TGF- β may control Foxo3a function *in vivo*. However, when we cultured LICs with TGF- β inhibitors in a stroma-free system, colony formation was not inhibited (Supplementary Fig. 25), suggesting that the survival and/or proliferation of LICs depends not only on TGF- β produced by LICs themselves but also on TGF- β in the surrounding microenvironment. Alternatively, TGF- β signalling in niche *in vivo* may affect LIC behaviour in a manner mediated by unknown factors. In any case, it appears that LICs are controlled by a complicated network of TGF- β signalling.

Although our study suggests that inhibition of the TGF- β -FOXO axis might represent a new therapeutic approach for CML patients, the application of TGF- β or FOXO inhibitors to the treatment of haematological malignancies warrants careful consideration (Supplementary Discussion 2). Our future work will be focused on further understanding how the LICs are maintained *in vivo*.

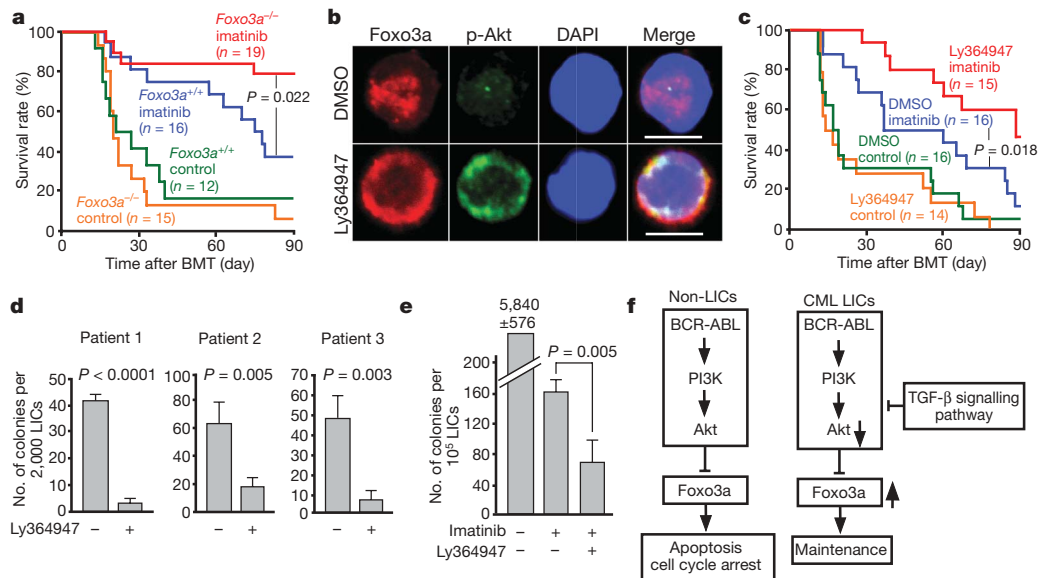


Figure 4 | Inhibition of TGF- β -Foxo3a signalling in combination with TKI therapy depletes CML *in vivo*. **a**, Foxo3a deficiency promotes the survival of imatinib-treated CML mice in a second BMT. At 10 days after BMT, mice transplanted with Foxo3a^{+/+} or Foxo3a^{-/-} LICs (1.5×10^4) received either vehicle (control) or imatinib for 80 days, and the percentage survival was determined. **b**, Ly364947 administration to CML-affected mice (25 mg kg⁻¹ for 7 days) increases p-Akt and decreases nuclear Foxo3a in LICs. Scale bars, 10 μ m. **c**, Combined administration of Ly364947 and imatinib prolongs the survival of CML-affected mice. At 10 days after BMT, recipients received

dimethyl sulphoxide (DMSO) or Ly364947 plus vehicle (control) or imatinib for 80 days, and the percentage survival was determined. **d, e**, Inhibition of TGF- β decreases the *in vitro* colony-forming ability of human CML LICs. CD34⁺CD38⁻Lin⁻ cells from bone marrow of CML patients were co-cultured on OP-9 cells with either DMSO (-) or Ly364947 (+) for 5 days in the absence (**d**) or presence (**e**) of imatinib. Data shown are the mean colony number \pm s.d. ($n = 3$). **f**, Scheme outlining the proposed distinct roles of Foxo3a in non-LICs versus CML LICs.

METHODS SUMMARY

For our mouse CML model, normal immature bone marrow cells (KLS⁺) from C57BL/6 mice were infected with retrovirus carrying MSCV-BCR-ABL-ires-GFP^{10,12,13}. The transduced KLS⁺ cells were transplanted intravenously into lethally irradiated (9.5 Gy) C57BL/6 congenic mice along with 5×10^5 bone marrow mononuclear cells from C57BL/6 mice. The development of CML-like MPD was confirmed by morphological analysis and marker determinations. To analyse phenotypes of LICs, the GFP⁺ KLS⁺ subpopulation from bone marrow and spleen was purified and transplanted into syngeneic recipients along with 5×10^5 bone marrow mononuclear cells. To examine Foxo3a in the maintenance of CML LICs, Foxo3a^{-/-} and Foxo3a^{+/+} littermates (C57BL/6; F4) were subjected to the above protocol. For Akt activity, TGF- β signalling and Foxo3a localization, freshly isolated GFP⁺KLS⁺ and KLS⁻ subpopulations, or GFP⁺KLS⁺ cells incubated for 2 h with 5 ng ml⁻¹ TGF- β 1 (R&D Systems) or 10 μ M Ly364947 (Merck), were immunostained with anti-p-Akt (Cell Signaling), anti-phospho-S6 (Cell Signaling), anti-phospho-Smad2/3 (Millipore), or anti-Foxo3a (Sigma). To examine colony-forming ability *in vitro*, GFP⁺KLS⁺ cells were cultured in semi-solid methylcellulose medium (stroma-free)¹⁵, or were co-cultured for 5 days on OP-9 stromal cells with Ly364947 (10 μ M). For experiments involving imatinib, GFP⁺KLS⁺ cells were cultured on OP-9 cells with or without 5 μ M imatinib (kind gift from Novartis), followed by washing and transfer to semi-solid medium. Human LICs were purified as CD34⁺CD38⁻Lin⁻ cells of bone marrow cells from CML patients (Cureline, Inc. and AllCells). These cells were co-cultured on OP-9 cells for 5 days before transfer to semi-solid medium. Cell cycling was assessed by *in vivo* BrdU incorporation (12 h). Apoptosis was assayed by TUNEL (Roche) or Annexin-V (Abcam) staining. Recipient mice bearing Foxo3a^{+/+} or Foxo3a^{-/-} CML LICs received either imatinib by oral gavage twice a day for 80 days at 200 mg kg⁻¹ (of body weight) per day, or Ly364947 by intraperitoneal administration for 80 days at 10 mg kg⁻¹ (of body weight) every 2 days.

Note added in proof: During the reviewing process, a paper demonstrating that human CML stem cells show predominant nuclear localization of FOXO proteins was published²⁵. The study supports our conclusion about the important roles of FOXO in CML LICs.

Full Methods and any associated references are available in the online version of the paper at www.nature.com/nature.

Received 9 March; accepted 4 December 2009.

Published online XX 2010.

- Ren, R. Mechanisms of BCR-ABL in the pathogenesis of chronic myelogenous leukaemia. *Nature Rev. Cancer* **5**, 172–183 (2005).

4

Nature nature08734.3d 23/12/09 13:38:10

- Komatsu, N. *et al.* A member of Forkhead transcription factor FKHL1 is a downstream effector of STI571-induced cell cycle arrest in BCR-ABL-expressing cells. *J. Biol. Chem.* **278**, 6411–6419 (2003).
- Ghaffari, S., Jagani, Z., Kitidis, C., Lodish, H. F. & Khosravi-Far, R. Cytokines and BCR-ABL mediate suppression of TRAIL-induced apoptosis through inhibition of forkhead FOXO3a transcription factor. *Proc. Natl Acad. Sci. USA* **100**, 6523–6528 (2003).
- Essafi, A. *et al.* Direct transcriptional regulation of Bim by FoxO3a mediates STI571-induced apoptosis in Bcr-Abl-expressing cells. *Oncogene* **24**, 2317–2329 (2005).
- Graham, S. M. *et al.* Primitive, quiescent, Philadelphia-positive stem cells from patients with chronic myeloid leukemia are insensitive to STI571 *in vitro*. *Blood* **99**, 319–325 (2002).
- Michor, F. *et al.* Dynamics of chronic myeloid leukaemia. *Nature* **435**, 1267–1270 (2005).
- Roeder, I. *et al.* Dynamic modeling of imatinib-treated chronic myeloid leukemia: functional insights and clinical implications. *Nature Med.* **12**, 1181–1184 (2006).
- Jørgensen, H. G., Allan, E. K., Jordanides, N. E., Mountford, J. C. & Holyoake, T. L. Nilotinib exerts equipotent antiproliferative effects to imatinib and does not induce apoptosis in CD34⁺ CML cells. *Blood* **109**, 4016–4019 (2007).
- Daley, G. Q., Van Etten, R. A. & Baltimore, D. Induction of chronic myelogenous leukemia in mice by the P210^{bcr/abl} gene of the Philadelphia chromosome. *Science* **247**, 824–830 (1990).
- Hu, Y. *et al.* Targeting multiple kinase pathways in leukemic progenitors and stem cells is essential for improved treatment of Ph⁺ leukemia in mice. *Proc. Natl Acad. Sci. USA* **103**, 16870–16875 (2006).
- Neering, S. J. *et al.* Leukemia stem cells in a genetically defined murine model of blast-crisis CML. *Blood* **110**, 2578–2585 (2007).
- Ito, K. *et al.* PML targeting eradicates quiescent leukaemia-initiating cells. *Nature* **453**, 1072–1078 (2008).
- Zhao, C. *et al.* Hedgehog signalling is essential for maintenance of cancer stem cells in myeloid leukaemia. *Nature* **458**, 776–779 (2009).
- Tothova, Z. *et al.* FoxOs are critical mediators of hematopoietic stem cell resistance to physiologic oxidative stress. *Cell* **128**, 325–339 (2007).
- Miyamoto, K. *et al.* Foxo3a is essential for maintenance of the hematopoietic stem cell pool. *Cell Stem Cell* **1**, 101–112 (2007).
- Yalcin, S. *et al.* Foxo3 is essential for the regulation of ataxia telangiectasia mutated and oxidative stress-mediated homeostasis of hematopoietic stem cells. *J. Biol. Chem.* **283**, 25692–25705 (2008).
- Yamazaki, S. *et al.* Cytokine signals modulated via lipid rafts mimic niche signals and induce hibernation in hematopoietic stem cells. *EMBO J.* **25**, 3515–3523 (2006).
- Pear, W. S. *et al.* Efficient and rapid induction of a chronic myelogenous leukemia-like myeloproliferative disease in mice receiving P210 bcr/abl-transduced bone marrow. *Blood* **92**, 3780–3792 (1998).

19. Yamazaki, S. *et al.* TGF- β as a candidate bone marrow niche signal to induce hematopoietic stem cell hibernation. *Blood* **113**, 1250–1256 (2009).
20. Massagué, J. TGF β in Cancer. *Cell* **134**, 215–230 (2008).
21. Sawyer, J. S. *et al.* Synthesis and activity of new aryl- and heteroaryl-substituted pyrazole inhibitors of the transforming growth factor- β type I receptor kinase domain. *J. Med. Chem.* **46**, 3953–3956 (2003).
22. Bhaskar, P. T. & Hay, N. The two TORCs and Akt. *Dev. Cell* **12**, 487–502 (2007).
23. Kodama, H., Nose, M., Niida, S. & Nishikawa, S. Involvement of the c-kit receptor in the adhesion of hematopoietic stem cells to stromal cells. *Exp. Hematol.* **22**, 979–984 (1994).
24. Møller, G. M., Frost, V., Melo, J. V. & Chantry, A. Upregulation of the TGF β signalling pathway by Bcr-Abl: implications for haemopoietic cell growth and chronic myeloid leukaemia. *FEBS Lett.* **581**, 1329–1334 (2007).
25. Pellicano, F. *et al.* FOXO transcription factor activity is partially retained in quiescent CML stem cells and induced by tyrosine kinase inhibitors in CML progenitor cells. *Blood*. doi:10.1182/blood-2009-06-226621 (1 December 2009).

Supplementary Information is linked to the online version of the paper at www.nature.com/nature.

Acknowledgements We thank H. Honda for BCR-ABL cDNA, C. A. Schmitt for MSCV-dnFoxo-ires-GFP, T. Nakamura for MSCV-NUP98-HOXA9, T. Kitamura for Plat-E retroviral packaging cells, T. Suda, N. Komatsu and K. Miyazono for discussions, and M. Sakae and T. Hatakeyama for expert technical support. We also thank Novartis International AG for imatinib (STI571). K.N. was supported by a grant-in-aid for Scientific Research (C), and A.H. was supported by grants-in-aid for Scientific Research (B) and Creative Scientific Research (17GS0419), from the Ministry of Education, Culture, Sports, Science and Technology, Japan.

Author Contributions K.N. designed research, performed experiments, analysed data, and co-wrote the paper. T.H., T.M., Y.T., T.O. and N.M. performed experiments. Y.K. and S.N. provided technical support for the human cell experiments. A.H. designed research, analysed data and co-wrote the paper.

Author Information Reprints and permissions information is available at www.nature.com/reprints. The authors declare no competing financial interests. Correspondence and requests for materials should be addressed to K.N. (kazunaka@kenroku.kanazawa-u.ac.jp) or A.H. (ahirao@kenroku.kanazawa-u.ac.jp).

METHODS

Mice. *Foxo3a*^{-/-} and littermate *Foxo3a*^{+/+} mice of the C57BL/6 (F4) genetic background¹⁵ were used in this study. C57BL/6 congenic mice were purchased from Sankyo-Lab Service. Animal care in our laboratory was in accordance with the guidelines for animal and recombinant DNA experiments of Kanazawa University. Imatinib (Glivec; purchased from Novartis) was administered to mice by oral gavage twice a day (200 mg kg⁻¹ of body weight per day in water). Ly364947 (Merck Chemicals Ltd) was prepared as a 5 mg ml⁻¹ stock solution in DMSO and intraperitoneally administered in saline to mice for 80 days at 10 mg kg⁻¹ (of body weight) every 2 days, or for 7 days at 25 mg kg⁻¹ (body weight) per day.

Flow cytometry and cell sorting. A FACSAria (BD Biosciences) and monoclonal antibodies recognizing the following markers were used for flow cytometry: Sca-1 (E13-161.7), CD4 (L3T4), CD8 (53-6.7), B220 (RA3-6B2), TER119 (Ly-76), Gr-1 (RB6-8C5), Mac1 (M1/70), IL7R α chain (B12-1), Fc γ III/II receptor (2.4G2) and CD34 (RAM34, Pacific blue-conjugated) (all from BD Biosciences). Anti-c-Kit (ACK2) monoclonal antibody was from eBiosciences. A mixture of monoclonal antibodies recognizing CD4, CD8, B220, TER119, Mac1 and Gr-1 was used to identify Lin⁺ cells.

Preparation of retrovirus. The cDNA encoding human *BCR-ABL* (gift from H. Honda) was cloned into the EcoRI site of the MSCV or MSCV-ires-GFP vector. Retroviral packaging cells (Plat-E) were transiently transfected with the MSCV-*BCR-ABL*-ires-GFP plasmid using FuGene6 reagent (Roche) and used for transplantation into mice as described later.

Generation of CML model and isolation of LIC population. Normal immature c-Kit⁺ Lin⁻ Sca-1⁺ haematopoietic cells (KLS⁺ cells) from *Foxo3a*^{-/-} and littermate *Foxo3a*^{+/+} mice were purified by flow cytometry and cultured in serum-free S-Clone SF-03 medium (Sanko Junyaku) supplemented with 10 ng ml⁻¹ human TPO (thrombopoietin; PeproTech) plus 10 ng ml⁻¹ mouse SCF (stem cell factor; Wako Pure Chemical). To generate our CML-like MPD mouse model, normal KLS⁺ cells were infected with the above retrovirus carrying MSCV-*BCR-ABL*-ires-GFP using CombiMag (OZ Bioscience). The transduced KLS⁺ cells were transplanted intravenously into lethally irradiated (9.5 Gy) C57BL/6 congenic mice along with 5 \times 10⁵ bone marrow mononuclear cells from C57BL/6 mice.

For the prospective isolation of LICs, mononuclear cells were isolated from bone marrow or spleen of CML-affected recipient mice at 12–14 days post-transplantation, and GFP⁺ subpopulations (3 \times 10⁴) were recovered by flow cytometric cell sorting, followed by transplantation into C57BL/6 congenic mice as described earlier. For serial transplantations, GFP⁺ KLS⁺ cells (3 \times 10⁴ or 1.5 \times 10⁴) were collected and pooled from five BMT mice and transplanted into a second set of lethally irradiated congenic recipient mice along with 5 \times 10⁵ normal bone marrow mononuclear cells from C57BL/6 mice. The absolute number of CML LICs in the spleen of a recipient mouse was calculated as (total number of mononuclear cells isolated from the bone marrow (two legs) or spleen \times frequency of GFP⁺ KLS⁺ cells (%) \times 1/100).

Mouse cell colony-forming assay. Mouse cells were cultured in semi-solid medium (stroma-free) containing the cytokines SCF, IL-3, IL-6 and erythropoietin¹⁵ (Methocult GF M3434; Stem Cell Technologies) at 37 °C in humidified air containing 5% CO₂ for 7 days. For co-culture assays, cells (1 \times 10³) were co-cultured on OP-9 stromal cells²³ under hypoxic conditions (5% O₂) for 5 days. After collecting and washing with PBS, colony formation was assessed in semi-solid medium as described earlier. For inhibition of TGF- β signalling, cells were co-cultured on OP-9 stromal cells in the presence of control (DMSO) or 2, 10 or 20 μ M Ly364947 or SD208 (Sigma) for 5 days, followed by washing and transfer to semi-solid medium. For the combination treatment of TGF- β inhibitor plus imatinib, cells were first treated with DMSO or a TGF- β inhibitor on OP-9 stromal cells. At 24 h after starting culture, the cells were treated with further DMSO or 5 μ M imatinib (STI571; provided by Novartis) and incubated for another 4 days (total 5 days). Thereafter, the cells were washed with PBS and transferred to semi-solid medium. The number of colonies was counted under the microscope.

Fluorescence immunostaining. Freshly isolated cells were incubated in S-Clone medium without cytokines for 30 min on poly-L-lysine (Sigma)-coated glass slides²⁶ at 37 °C under hypoxic conditions (5% O₂). To examine the effects of TGF- β signalling, cells were treated with 5 ng ml⁻¹ TGF- β 1 (R&D Systems), 10 μ M Ly364947 (Merck), or vehicle control at 37 °C for 2 h. After fixation with 4% paraformaldehyde for 30 min and permeabilization with 0.25% Triton X-100 for 2 min, the cells were blocked by incubation in 2% BSA/PBS for 1 h. For immunostaining, the permeabilized cells were incubated with mouse or rabbit anti-FKHRL1 (Foxo3a) (FR1 or F2178; Sigma), rabbit anti-Foxo4 (9472; Cell Signaling), rabbit anti-phospho-Smad2/3 (Millipore), rabbit anti-phospho-Akt (D9E; Cell Signaling), or rabbit anti-phospho-S6 ribosomal protein (2211;

Cell Signaling) antibodies at 4 °C for 12 h. Primary antibodies were visualized by incubating the cells with AlexaFluor 546- or AlexaFluor 647-conjugated goat anti-mouse IgG or goat anti-rabbit IgG (Molecular Probes). Nuclei were stained with the DNA marker DAPI (Sigma). Stained slides were mounted using Fluoromount Plus (Diagnostic Biosystems), and fluorescent images were acquired using a Fluoview 1000 laser confocal microscope (Olympus) and Photoshop software (Adobe). Fluorescence intensities were quantified using ImageJ software. To evaluate the subcellular localization of Foxo3a, approximately 100 cells per group were counted under the microscope.

Cell cycle analysis and differentiation potential. To determine the cell cycle status of LICs *in vivo*, second BMT CML mice were administered BrdU intraperitoneally (100 mg kg⁻¹ of body weight in saline; Sigma) for 12 h. Numbers of BrdU⁺ LICs were assessed by immunostaining with anti-BrdU antibody (3D4; BD Biosciences) and flow cytometry. To examine the cell cycle status of LICs *in vivo* and determine the nuclear localization of Foxo3a, cells were co-stained with rabbit anti-FKHRL1 antibody (F2178; Sigma) to detect Foxo3a, and anti-mouse Ki67 antibody (B56; BD Biosciences).

To evaluate differentiation potential, the frequencies of CMP-like (CD34⁺Fc γ III/II receptor⁻), GMP-like (CD34⁺Fc γ III/II receptor⁺), and MEP-like (CD34⁻Fc γ III/II receptor⁻) cells among GFP⁺ bone marrow cells obtained from *Foxo3a*^{+/+} and *Foxo3a*^{-/-} CML mice at first BMT were analysed by flow cytometry.

Detection of apoptosis. To determine apoptosis *in vivo*, freshly isolated spleens and bones were immediately fixed with 4% paraformaldehyde, and tissue sections were prepared and stained using the TUNEL method (Roche). Isolated GFP⁺KLS⁺ cells from mice that had been transplanted with *Foxo3a*^{+/+} and *Foxo3a*^{-/-} CML LICs (second BMT) were either co-stained with Annexin-V-PECy5 (Abcam) and examined by flow cytometry, or stained *in vitro* using the TUNEL method (Roche).

Inhibition of endogenous Foxo by dominant-negative Foxo. Retroviruses carrying a dominant negative (dn)Foxo vector (MSCV-dnFoxo-ires-GFP²⁷) or a control GFP vector (MSCV-ires-GFP) were generated as described earlier. To obtain dnFoxo CML LICs, normal KLS⁺ cells (wild-type C57BL/6 CD45.1) were infected with retrovirus carrying the *BCR-ABL* gene (without GFP). These infected KLS⁺ cells were transplanted into irradiated recipient mice (C57BL/6 CD45.2). At 14 days after transplantation, donor-derived KLS⁺ cells were isolated and infected with retrovirus carrying the control GFP or dnFoxo-ires-GFP vector. To examine the reconstitution of CML LICs *in vivo*, retrovirus-infected CML LICs (unfractionated) were transplanted intravenously into lethally irradiated C57BL/6 congenic mice along with 5 \times 10⁵ bone marrow mononuclear cells from C57BL/6 mice. At 14 days after transplantation, absolute numbers of GFP⁺KLS⁺ cells were measured in recipient spleens. To examine LIC colony-forming ability *in vitro*, these GFP⁺ CML LICs were cultured in semi-solid medium (stroma-free), or were co-cultured on OP-9 stromal cells as described earlier.

Quantitative real-time RT-PCR analysis. RNA samples were purified from fractionated GFP⁺KLS⁺ and GFP⁺KLS⁻ cells (1.0 \times 10⁵) using the RNeasy kit (QIAGEN) and reverse-transcribed using the Advantage RT-for-PCR kit (Takara-Clontech). Real-time quantitative PCR was performed using SYBR green Premix EX Taq (Takara) on an Mx3000P Real-time PCR system (Stratagene). The following primers were used: *Tgfb1*, 5'-TATGCTAAAGAGGTCACCCGCG-3' and 5'-TGCTTCCCGAATGTCTGACG-3'; *Alk5* (also known as *Tgfb1*), 5'-GATCGCCCTTTCATTTGAGAGG-3' and 5'-AAACCGACCTTTCGCAATGC-3'; *Tgfb2*, 5'-GAGAGCATGAAAGACAGTGTGC-3' and 5'-CCAGCACTCGGTC AAAGTCT-3'; *Actb*, 5'-AGGTCATCACTATTGGCAACGA-3' and 5'-CACTT CATGATGGAATTGAATGTAGTT-3'. The following cycle parameters were used: denaturation at 95 °C for 10 s, and annealing and elongation at 57 °C for *Actb*, and 60 °C for *Tgfb1*, *Tgfb1* and *Tgfb2*.

Analyses of primary human CML samples. Viable bone marrow mononuclear cells from patients with chronic phase CML were purchased from Cureline, Inc. (no. 16-122); and AllCells LLC (no. 06-255 and 06-620). Cells were stained with anti-CD34 (8G12), anti-CD38 (HIT2), anti-CD3 (SK7), anti-CD16 (3G8), anti-CD19 (SJ25C1), anti-CD20 (L27), anti-CD14 (M ϕ P9), and anti-CD56 (NCAM16.2) antibodies (all from BD Biosciences). A mixture of monoclonal antibodies recognizing CD3, CD16, CD19, CD20, CD14 and CD56 was used to identify Lin⁻ cells. CD34⁺CD38⁻Lin⁻ cells were purified by cell sorting. To examine the effects of treatment with Ly364947 alone or a combination of Ly364947 plus imatinib, CD34⁺CD38⁻Lin⁻ cells were cultured on OP-9 stromal cells as described earlier. After collecting and washing in PBS, the colony-forming ability of LICs was evaluated by culture in semi-solid medium containing SCF, GM-CSF, IL-3, IL-6, G-CSF and erythropoietin (Methocult GF⁺ H4435; Stem Cell Technologies).

Generation of CML blast crisis model. A mouse model of CML blast crisis was generated as previously described²⁸. In brief, normal KLS⁺ cells were co-infected with a retrovirus carrying MSCV-*BCR-ABL*-ires-GFP and a retrovirus carrying

MSCV-NUP98/HOXA9. The transduced Lin⁻Sca-1⁺ (LS⁺) cells¹¹ were transplanted intravenously into lethally irradiated C57BL/6 congenic mice along with 5×10^5 bone marrow mononuclear cells from C57BL/6 mice.

Statistical analyses. Statistical differences were determined using the unpaired Student's *t*-test for *P*-values, and the long-rank non-parametric test for survival curves.

26. Ema, H. *et al.* Adult mouse hematopoietic stem cells: purification and single-cell assays. *Nature Protocols* **1**, 2979–2987 (2006).
27. Bouchard, C. *et al.* FoxO transcription factors suppress Myc-driven lymphomagenesis via direct activation of Arf. *Genes Dev.* **21**, 2775–2787 (2007).
28. Dash, A. B. *et al.* A murine model of CML blast crisis induced by cooperation between BCR/ABL and NUP98/HOXA9. *Proc. Natl Acad. Sci. USA* **99**, 7622–7627 (2002).

Author Queries

Journal: **Nature**

Paper: **nature08734**

Title: **TGF- β -FOXO signalling maintains leukaemia-
?initiating cells in chronic myeloid leukaemia**

Query Reference	Query
1	AUTHOR: When you receive the PDF proofs, please check that the display items are as follows (doi:10.1038/nature08734): Figs 1–4 (colour); Tables: None; Boxes: None. Please check all figures very carefully as they have been re-labelled, re-sized and adjusted to Nature's style.
2	Nature Proofreader: Please update/confirm the tentative publication date

For Nature office use only:

Layout	<input type="checkbox"/>	Figures/Tables/Boxes	<input type="checkbox"/>	References	<input type="checkbox"/>
DOI	<input type="checkbox"/>	Error bars	<input type="checkbox"/>	Supp info (if applicable)	<input type="checkbox"/>
Title	<input type="checkbox"/>	Colour	<input type="checkbox"/>	Acknowledgements	<input type="checkbox"/>
Authors	<input type="checkbox"/>	Text	<input type="checkbox"/>	Author contribs (if applicable)	<input type="checkbox"/>
Addresses	<input type="checkbox"/>	Methods (if applicable)	<input type="checkbox"/>	COI	<input type="checkbox"/>
First para	<input type="checkbox"/>	Received/Accepted	<input type="checkbox"/>	Correspondence	<input type="checkbox"/>
Display items	<input type="checkbox"/>	AOP (if applicable)	<input type="checkbox"/>	Author corr	<input type="checkbox"/>